Influence of annealing temperatures on the properties of low aspect-ratio TiO_2 nanotube layers

Sayantan Das[a], Raul Zazpe[a], Jan Prikryl[a], Petr Knotek[b], Milos Krbal[a], Hanna Sopha[a,1], Veronika Podzemna[a], Jan M. Macak[a,*,1]

[a]*Center of Materials and Nanotechnologies, Faculty of Chemical Technology, University of Pardubice, Nam. Cs. Legii 565, 53002 Pardubice, Czech Republic*

[b] *Dep. of General and Inorganic Chemistry, Faculty of Chemical Technology, University of Pardubice, Studentská 573, 53210 Pardubice, Czech Republic*

**Corresponding Author: e-mail: jan.macak@upce.cz,* Phone: +420 466 037 401

[1] ISE member

Abstract

The present work reports on the effect of thermal annealing on electrical, optical and structural properties of low aspect ratio self-organized TiO_2 nanotube layers formed by anodization of Ti. The average inner diameter and length of the nanotubes was 100 nm and 1 µm, respectively. From the whole range of temperatures (300-600 °C), annealing at 400 ^oC leads to the formation of crystalline TiO_2 nanotube layers with anatase structure offering best electrical and photo-electrochemical properties. Conducting atomic force microscopy studies have been explored for the first time to identify the annealing temperature of nanotube TiO_2 layers with best electrical properties.

Keywords: TiO_2 nanotubes; anodization; annealing; anatase; rutile

1. Introduction

Scientific utilization of nanotubular titanium dioxide (TiO_2) layers prepared by anodization of Ti has increased immensely since pioneering works [1-3]. Other transition metal oxides are also known to form nanotubular arrangements, however, TiO_2 has attracted most widespread attention [4, 5]. The attractiveness of TiO_2 nanotubes stems not only from their unique one dimensional (1D) architecture but also from the wide range of their specific physical and chemical properties [4, 5]. These features of make TiO_2 nanotubes useful in many applications ranging from biomedical [6], gas sensing [7] to photon assisted water splitting [8], photocatalysis [9] and in different types of solar cell devices including organic/polymer [10], dye-sensitized [11] and perovskite based solar cells [12]. TiO_2 is an *n*-type semiconductor with a bandgap energy, E_g ~ 3.2 eV for anatase and E_g ~ 3.0 eV for the rutile phase, and it represents the most widely used material for photo-electrochemical applications owing to its low cost, non-toxicity and stability against photo-corrosion [13-16]. TiO_2 nanotube structures with various morphologies can be grown on Ti substrates by anodic oxidation in fluoride-containing electrolytes with optimized anodization conditions to obtain tubes with particular diameters and thicknesses [4, 5]. The self-organized arrays of TiO_2 nanotubes attached perpendicular to the Ti substrate represent a very favorable architecture especially for photo-electrochemical studies. Other than providing high surface area and enhanced light absorption in their 1D ordered structure, the straight nanotubular wall also offer the most direct path for photo-generated electrons towards the underlying Ti metal back contact [17]. Moreover, proper annealing treatment of the TiO_2 nanotubes is of utmost importance for controlling the crystalline state of the nanotubes, as the efficiency of different chemical and physical reactions can be significantly improved by carefully developing the anatase or rutile phase [18, 19].

There are several reports that show an influence of the annealing atmosphere and temperature on the crystallinity of the nanotubes and their subsequent photo-electrochemical performance [18-23]. However, according to our best knowledge no studies have yet reported the comparison of different annealing temperatures with the photo-electrochemical, electrical and structural properties of low aspect-ratio TiO_2 nanotube layers with thickness around 1 μm. Beside the efforts that were carried out within past 10 years to develop a high aspect ratio nanotube layers, the lower aspect ratio nanotube layers presented in this work have recently found uses as anodes in perovskite solar cells [12, 24, 25]. Thus, it is of very high importance to explore properties of these nanotubes. The anatase structure of TiO_2 is the most favorable phase for both photo-electrochemical and catalytic studies because this phase demonstrates maximum electron mobility [26-28]. Previous investigations revealed that anatase TiO_2 nanotube layers can be obtained by annealing the nanotube layers between 400-500 ^{o}C [17-23].

Therefore, in this paper we present a series of relevant investigations of 1 μm thick TiO_2 nanotube layers annealed at different temperatures in air. We aim to obtain more insights into the influence of annealing temperature on some key parameters of TiO_2 nanotubes, such as morphology, structure, energy bandgap, electrical resistance and photo-electrochemical properties. In particular, we describe in detail morphological changes due to an additional thermally grown TiO_2 layer in between the nanotube layer and Ti substrate. Further, we also show for the first time electrical resistance measurement of the nanotube layers by conductive atomic force microscopy (c-AFM) technique.

2. Experimental details

Prior to anodization, the Ti foils (Sigma-Aldrich 0.127 mm thick, 99.7% purity) were degreased by sonication in isopropanol and acetone followed by rinsing with isopropanol and

drying in air. The clean Ti foils (working electrodes) were pressed against an O-ring of the electrochemical cell, leaving a circular area of 1 cm^2 open to the electrolyte. The electrochemical setup consisted of a two electrode configuration and used a platinum foil as the counter electrode. Electrochemical experiments were carried out at room temperature engaging a high-voltage potentiostat (PGU-200V, IPS Elektroniklabor GmbH). A glycerol/deionized water mixture (50:50 vol.%) containing 270 mM NH_4F were used as electrolyte [29]. Ti foils were anodized at 20 V for 100 min after sweeping the potential from 0 V to 20 V with a sweeping rate of 1 V/s. After anodization the foils were rinsed and sonicated in isopropanol and dried.

The TiO_2 nanotube layers obtained after anodization were annealed in a muffle oven. Layers were placed inside the oven at room temperature followed by heating the oven at 15^oC/min rate. Once the target annealing temperature was reached, the annealing was performed for 3 hours. After the annealing time was over the heating power turned off and the layers cooled down inside the oven to room temperature. The annealing temperatures were 300 ^oC, 400 ^oC, 500 ^oC and 600 ^oC.

For the structural and morphological characterization of the nanotube layers, top-view and cross-sectional observations were carried out by a field-emission electron microscope (FE-SEM JEOL JSM 7500F). Diffraction analyses were also carried out using X-ray diffractometer (D8 Advance, Bruker AXE) using CuKα radiation with secondary graphite monochromator and Na(Tl)I scintilation detector.

The electrical resistance of TiO_2 nanotube layer was analysed by two techniques: i) two-point probe (Au-coated W tips on the nanotube layer and the back contact to Ti foil, both interfaced to the digital multimeter Keithley 2602) and ii) conductive atomic force microscope (c-AFM, Solver Pro M, NT-MDT), where the conductive AFM tip was placed on

the top of the nanotube wall [30]. Photo-electrochemical investigations were carried out in 0.1 M Na_2SO_4 using a photo-electrochemical setup (Instytut Fotonowy) based on monochromatized Xe lamp, Autolab potentiostat (PGSTAT 204, Metrohm Autolab) and a three-electrode cell equipped with a flat quartz window. The electrodes were contacted and then pressed against an O-ring of a photo-electrochemical cell leading to an irradiated area of 0.28 cm^2. A platinum wire served as a counter electrode and Ag/AgCl (3M KCl) as a reference electrode. To evaluate the photoresponse, photocurrent transients were recorded at a constant potential of 0.4 V (vs. Ag/AgCl) using a tunable light source provided with 150 W xenon lamp and a universal grating monochromator. Monochromatic light employed for excitation was chopped with light and dark phases of 10 s each and a step of 5 nm.

3. Results and Discussion

Figure 1 shows FE-SEM images of amorphous TiO_2 nanotube layer prepared by anodization of Ti foil in water: glycerol (50:50 vol.%) electrolyte containing 270 mM NH_4F. As shown in Fig. 1a, the nanotube layer consists of moderately ordered and densely packed nanotubes. The cross-sectional image (Fig. 1b) was obtained from a mechanically bent Ti foil where a lift of the nanotube layer occurred. Analysis of the images (top view and cross-sectional view) revealed that the average diameter and the length of the nanotubes were ~100 nm and ~1 μm, respectively. Thus, the resulting aspect-ratio of these layers was ≈ 10. Unlike the hydrothermal process, TiO_2 nanotubes prepared by the anodization process are amorphous in nature [17-23]. However, as anatase is at large the most preferred crystal structure for numerous electron-conducting applications, such as dye-sensitized solar cells or photocatalytic electrodes, a proper annealing technique needs to be employed to obtain only anatase structure.

Figure 2 shows the top view SEM images of tubes annealed at 300 ^{o}C, 400 ^{o}C, 500 ^{o}C and 600 ^{o}C. From these images, it is clear that no drastic morphological changes appear in the nanotubular structure after thermal treatment. Nevertheless, with increase in the annealing temperature, it was observed that rims of the tubes become thicker and more rounded, as shown in inset images of Fig. 2. In addition, Fig. 3 shows cross-sectional images of nanotube layers shown in Fig. 2. An important effect of annealing is shown in Fig. 3. When the regions at bottom of the tube layers were analyzed closely with FESEM (shown in Fig. 3a-d) the presence of an additional oxide layer underneath the tubes was observed in all cases. This reveals that the annealing treatment results in the growth of some direct thermal oxide underneath the nanotube layers. Due to heat transfer reasons, crystallization of anodized TiO_2 nanotube layers in conventional furnaces starts from the underlying Ti substrate. It can be seen that the tubes annealed at 300 ^{o}C and 400 ^{o}C illustrates a growth of ~30 nm and ~80 nm thick thermal oxide at the bottom of the tubes. However, a substantial thermal oxide layer growth was observed for layers annealed at 500 ^{o}C and 600 ^{o}C. The average thickness of these layers were about 150 nm and 350 nm for layers annealed at 500 ^{o}C and 600 ^{o}C, respectively. To the best of our knowledge, this increase of thickness of the thermal oxide at wider range of temperature has not been demonstrated earlier, though this oxide formation underneath the nanotube layer was already revealed upon annealing at particular temperatures only [21, 31]. It should also be noted that Jaroenworaluck et al. showed that TiO_2 nanotube layers with thickness around ~1.5 μm collapse after annealing at 500 and 600 ^{o}C [32]. However, in our study we annealed ~1 μm thick nanotube layers to temperatures as high as 600 ^{o}C and successfully kept the nanotube structure intact as can be seen in Figs. 2 and 3. The thicknesses of tube walls of nanotube layers in the present paper and in Ref. [32] were statistically compared, revealing an average wall thickness of 25 and 10 nm, respectively.

Thus, the higher temperature stability of the nanotube layers in this paper can be assigned to an increased robustness of the nanotubes.

As mentioned earlier (and as widely supported by existing literature [17-23]), TiO_2 nanotubes obtained by anodization process are amorphous in nature, so XRD was performed only on annealed nanotubes. Albu et al. suggested that the TiO_2 layer formed after annealing at 350 and 450 ^oC at the bottom of the nanotubes consists mainly of rutile phase, whereas the tube walls consists of anatase [28]. Figure 4 shows XRD patterns for nanotube layers annealed at 300 ^oC, 400 ^oC, 500 ^oC and 600 ^oC for 3 hours. According to the crystallographic database, the (101) peak for the anatase TiO_2 structure is expected at $2\theta = 25.4^o$ (JCPDS card, No. 21-1271). Closer analysis shows that the intensity of the anatase (101) peak increases from 300 ^oC to 400 ^oC. However, for layers annealed at 600 ^oC the anatase (101) peak intensity decreases and the rutile (110) and (101) peaks at $2\theta = 27.5^o$, 36.1^o (JCPDS card, No. 21-1276), respectively, starts to appear. At this temperature, it is very likely that the tubes undergo some anatase to rutile phase transformation. The crystallite size of anatase (101) crystals, evaluated from XRD patterns using Scherrer's formula [33] for layers annealed at different temperatures are illustrated in Table 1. It also shows that rutile (110) grains appear only for the layers annealed at 600 ^oC.

The value of photocurrent density was taken as a difference between current density under irradiation and in the dark. The incident photon-to-current efficiency (IPCE) for each wavelength was calculated according to the equation:

$$\mathrm{IPCE}(\%) = \frac{i_{ph} h\nu}{Pq} \times 100 \qquad (1)$$

where, i_{ph} is the photocurrent density, h is Planck's constant, v is light frequency, P is the light power density, and q is the charge of an electron.

Figures 5a-d shows IPCE plots for TiO_2 nanotubes annealed at different temperatures for 3h. It is apparent that in the UV light region, layers annealed at 400 ^oC provide highest IPCE values. This difference can be described in terms of impact from anatase and rutile phases of TiO_2. The bandgap of the anatase phase is ~3.2 eV, but it has a higher electron conductivity than the rutile phase [34-35]. In contrast, rutile has a bandgap of ~3.0 eV. Therefore, it can be hypothesized that at short wavelength, shorter than 340 nm, the anatase phase with higher electron mobility (lower recombination) results in overall higher IPCE values. This is particularly apparent from comparison of IPCE values of nanotube layers annealed between 400 °C and 600 °C, where nanotube layers that were annealed at 600 °C showed a strong decrease of IPCE values. The lower IPCE values obtained from nanotube layers annealed at 600 °C were due to increased rutile content in the TiO_2 nanotube layer (as can be seen from XRD results, Fig. 4), as well as due to the growth of a thick thermal oxide layer underneath the tubes (as evidenced in Fig. 3d).

The insets in Figure 5 show $(IPCE.hv)^{1/2}$ versus hv plots which were utilized to explore the influence of annealing on the indirect band gap energy, E_g, of TiO_2 nanotubes [17, 34, 35]. The linear part of this curve indicates a transition above an optical band-edge and the x-intercept corresponds to the bandgap energy of the TiO_2 nanotube layers. The band gap energies are compiled in Table 1. All the results for bandgap shifts with increase in annealing temperature can be explained by rutile formation, i.e. as the annealing temperature increases, rutile content increases and the bandgap value decreases. The grain size change as illustrated in Table 1 shows that with an increase in the annealing temperature, the anatase grain size also increases. However, the rutile grains only appeared in layers annealed at 600 ^oC with a grain size of 61.5 nm as determined by the Scherrer's equation [33]. Although the anatase grain size increases after annealing at 600 ^oC, the presence of a thick thermal oxide

layer underneath the tubes acts as a barrier to the flow of electron towards the Ti back contact, thus drastically reducing the photocurrents and hence lower IPCE values.

To obtain a deeper knowledge about the nanotube layers, their electrical resistance after annealing at different temperatures was determined by c-AFM studies and conventional two-point probe measurement. Figure 6a shows that the tube layers annealed at 400 ^{o}C have the lowest resistance among the others involved in this study, regardless of the type of measurement. The resistance of the tubes annealed at 300 ^{o}C shows a resistance of the order of 10^9 ohms and 5×10^5 ohms, when measured by c-AFM and two-point probe technique, respectively. The layers annealed at 500 °C or 600 °C showed a significant increase in the resistance values and were recorded on the order of 10^8 – 10^9 ohms. This increased resistance might be due to the growth of thermal oxide layer underneath the tubes (shown in Fig. 3) or the presence of rutile phase (with lower electron mobility) within the nanotubes or combination of both the factors.

The differences in resistance values obtained by both techniques became smaller at higher temperatures. This difference can be explained as follows. For the c-AFM measurements, two or maximum three surrounding nanotubes were measured, depending on the exact position of very sharp tip (few nm diameters at the end of the tip, leaving few nm^2 of the contact area [30]), whereas by the two-point probe measurements, several hundreds of nanotubes are were contact with the tip (represented by an area of approx. 20 µm^2, as verified by SEM). The difference in contact area of both tips with the nanotube layers is schematically depicted in Figure 6b and 6c for two different temperatures – 300 °C and 600 °C, respectively.

In addition, morphological circumstances came into play here. For the nanotube layers annealed at 300°C, as shown in Figure 6d, and partially also at 400 °C and 500 °C, numerous nanotubes have on the very uppermost parts clearly visible rings (resulting from TiO_2

oxidation and dissolution events occurring during the nanotube growth) that are in a loose contact with the rest of the nanotube bodies. On the other hand, nanotubes at 600 °C, as shown in Figure 6e, do not contain any loose ring, as they melt at this very high temperature (in contrast to more robust nanotube bodies). In practice, the electrical contact between the c-AFM tip and the tube uppermost part is established as soon as the AFM tip touches any solid material as the first contact/touch - in our case with a tube part. When such loose ring, as shown in Figure 6d, is being contacted by c-AMF, rather very high resistivity is recorded via this very small spot, compared to the case, when the regular nanotube opening (loose-ring-free, shown in Figure 6e) gets in contact with the c-AFM tip. In contrast, the electrical contact between the Au-coated W tip of two-point probe measurement and nanotube uppermost parts spans over many more tubes. Thus, this contact is always very solid, independently on the annealing temperature. However, within c-AMF measurements, it was experimentally not plausible to distinguish between the good and loose points of the nanotubes. Thus the overall resistances were higher compared to the two-point probe measurements, provided that the higher the temperatures, the differences become smaller and smaller. All in all, it has to be pointed out that the trends observed in both of these measurement exactly matched with the trends of resistance values previously published for different aspect ratio nanotubes and annealing treatments carried out in different atmospheres [22, 23].

4. Conclusions

In the present work, we have explored several different features of self-organized TiO_2 nanotubes layers with thickness of approx. 1 μm, produced in mixed water-glycerol electrolyte with 270 mM NH_4F content. We showed that annealing TiO_2 nanotubes under oxidizing conditions results in the formation of anatase crystal structure in the temperature range of ~300 - 500 ^oC, while at temperatures around 600 ^oC, a mixture of anatase and rutile

phase was revealed. Crystallization and growth of thermal oxide layer starts from the metallic substrate that acts as a main heat sink. With increase in the annealing temperature, mainly due to the growth of thick rutile layer, the mobility of electrons decreased resulting in lower IPCE values. Layers annealed at 500 ^{o}C showed significant increase in the grain size; however, at this temperature, there was a considerable growth of a thick thermal oxide underneath the tubes which contributes to the decrease in the IPCE values. From all investigated temperatures, the nanotube layers annealed at 400 °C showed the best photo-electrochemical results and the lowest resistivity. All in all, we believe that the present results provide an important source of information for further utilization of nanotube layers, especially in photo-electrochemical and electrical applications.

Acknowledgements

European Research Council (ERC) and the Ministry of Education, Youth and Sports of the Czech Republic, are acknowledged for their financial support through projects 638857 and LM2015082, respectively.

References

[1] M. Assefpour-Dezfuly, C. Vlachos, E. H. Andrews, Oxide morphology and adhesive bonding on titanium surfaces, J. Mater. Sci. 19 (1984) 3626-3639.

[2] V. Zwilling, E. Darque-Ceretti, A. Boutry-Forveille, D. David, M. Y. Perrin, M. Aucouturier, Structure and physicochemistry of anodic oxide films on titanium and TA6V alloy, Surf. Interf. Anal. 27 (1999) 629-637.

[3] R. Beranek, H. Hildebrand, P. Schmuki, Self-organized porous titanium oxide prepared in H_2SO_4/HF electrolytes, Electrochem. Solid-State Lett. 6 (2003) B12-B14.

[4] J. M. Macak, H. Tsuchiya, A. Ghicov, K. Yasuda, R. Hahn, S. Bauer, P. Schmuki, TiO_2 nanotubes: Self organized electrochemical formation, properties and applications, Curr. Opin. Solid State Mater. Sci. 11 (2007) 3-18.

[5] K. Lee, A. Mazare, P. Schmuki, One-dimensional titanium dioxide nanomaterials: Nanotubes, Chem. Rev. 114 (2014) 9385–9454.

[6] S. Bauer, J. Park, J. Faltenbacher, S. Berger, K. von der Mark, P. Schmuki, Size selective behavior of mesenchymal stem cells on ZrO_2 and TiO_2 nanotube arrays, Integr. Biol., 1 (2009) 525-532.

[7] P. M. Perillo, D. F. Rodriguez, The gas sensing properties at room temperature of TiO_2 nanotubes by anodization, Sensor. Actuat. B-Chem, 171 (2012) 639-643.

[8] G.K. Mor, K. Shankar, M. Paulose, O.K. Varghese, C.A. Grimes, Enhanced photocleavage of water using titania nanotube arrays, Nano Lett. 5 (2009) 191-195.

[9] J. M. Macak, M. Zlamal, J. Krysa, P. Schmuki, Self-organized TiO_2 nanotube layers as highly efficient photocatalysts, Small, 3 (2007) 300-304.

[10] D. Pugliese, A. Lamberti, F, Bella, A. Sacco, S. Bianco, E. Tresso, TiO_2 nanotubes as flexible photoanode for back-illuminated dye-sensitized solar cells with hemi-squaraine

organic dye and iodine-free transparent electrolyte, Org. Electron., 15 (2014) 3715-3722.

[11] P. Roy, D. Kim, K. Lee, E. Spiecker, P. Schmuki, TiO_2 nanotubes and their application in dye-sensitized solar cells, Nanoscale 2 (2010) 45-59.

[12] X. Gao, J. Li, J. Baker, Y. Hou, D. Guan, J. Chen, C. Yuan, Enhanced photovoltaic performance of perovskite $CH_3NH_3PbI_3$ solar cells with freestanding TiO_2 nanotube array films, Chem. Commun. 50 (2014) 6368-6371.

[13] M. R. Hoffmann, S. T. Martin, W. Choi, D. W. Bahnemann, Environmental applications of semiconductor photocatalysis, Chem. Rev. 95 (1995) 69-96.

[14] A. Fujishima, T. N. Rao, D. A. Tryk, Titanium dioxide photocatalysis, J. Photochem. Photobiol. C, 1 (2000) 1-21.

[15] D. A. Tryk, A. Fujishima, K. Honda, Recent topics in photoelectrochemistry: achievements and future prospects, Electrochim. Acta 45 (2000) 2363-2376.

[16] O. Carp, C. L. Huisman, A. Reller, Photoinduced reactivity of titanium dioxide, Prog. Solid State Chem. 32 (2004) 33-177.

[17] R. Beranek, H. Tsuchiya, T. Sugishima, J. M. Macak, L. Taviera, S. Fujimoto, H. Kisch, P. Schmuki, Enhancement and limits of photoelectrochemical response from anodic TiO_2 nanotubes, App. Phys. Lett. 87 (2005) 243114-243116.

[18] H. Tsuchiya, J. M. Macak, A. Ghicov, A. S. Rader, L. Taveira, P. Schmuki, Characterization of electronic properties of TiO_2 nanotubes, Corros. Sci. 49 (2007) 203-210.

[19] D. Regonini, A. Jaroenworaluck, R. Stevens, C.R. Bowen, Effect of heat treatment on the properties and structure of TiO_2 nanotubes: phase composition and chemical composition, Surf. Interface Anal. 42 (2010) 139-144.

[20] J. M. Macak, S. Aldabergerova, A. Ghicov, P. Schmuki, Smooth anodic TiO_2 nanotubes: annealing and structure, Phys. Stat. Sol. (a) 203 (2006) R67-R69.

[21] A. Ghicov, H. Tsuchiya, J. M. Macak, P. Schmuki, Annealing effects on the photoresponse of TiO_2 nanotubes, Phys. Stat. Sol. (a) 203 (2006) R28-R30.

[22] A. Tighineanu, S. P. Albu, P. Schmuki, Conductivity of anodic TiO_2 nanotubes: Influence of annealing conductions, Phys. Stat. Sol. RRL 8 (2014) 158-164.

[23] A. Tighineanu, T. Ruff, S. P. Albu, R. Hahn, P. Schmuki, Conductivity of anodic TiO_2 nanotubes: Influence of annealing time and temperature, Chem. Phys. Lett. 494 (2010) 260-263.

[24] X. Wang, Z. Li, W. Xu, S. A. Kulkarni, S. K. Batabyal, S. Zhang, A. Cao, L. H. Wong, TiO_2 nanotube arrays based flexible perovskite solar cells with transparent carbon nanotube electrode, Nano Energy 11 (2015) 728-735.

[25] R. Salazar, M. Altomare, K. Lee, J. Tripathy, R. Kirchgeorg, N. T. Nguyen, M. Mokhtar, A. Alshehri, S. A. Al-Thabati, P. Schmuki, Use of anodic TiO_2 nanotube layers as mesoporous scaffolds for fabricating $CH_3NH_3PbI_3$ perovskite-based solid-state solar cells, ChemElectroChem, 2 (2015) 824-828.

[26] H. Tang, K. Prasad, R. Sanjines, P. E. Schmid, F. Levy, Electrical and optical properties of TiO_2 anatase thin films, J. Appl. Phys. 75 (1994) 2042-2047.

[27] L. Forro, O. Chauvet, D. Emin, L. Zuppiroli, H. Berger, F. Levy, High mobility n-type charge carriers in large single crystals of anatase (TiO_2), J. Appl. Phys. 75 (1994) 633-635.

[28] X. Liu, P. K. Chu, C. Ding, Surface modification of titanium, titanium alloys, and related materials for biomedical applications, Mater. Sci. Eng. R47 (2004) 49-121.

[29] J. M. Macak, H. Hildebrand, U. Marten-Jahns, P. Schmuki, Mechanistic aspects and growth of large diameter self-organized TiO_2 nanotubes, J. Electroanal. Chem. 621 (2008) 254

[30] P. Knotek, J. Taseva, K. Petkov, M. Kincl, L. Tichy, Optical properties and scanning probe microscopy study of some Ag-As-S-Se amorphous films, Thin Solid Films 517 (2009) 5943-5947.

[31] S. P. Albu, H. Tsuchiya, S. Fujimoto, P. Schmuki, TiO_2 nanotubes-annealing effects on detailed morphology and structure, Eur. J. Inorg. Chem. 2010 (2010) 4351-4356.

[32] A. Jaroenworaluck, D. Regonini, C.R. Bowen, R. Stevens, A microscopy study of the effect of heat treatment on the structure and properties of anodised TiO_2 nanotubes, Appl. Surf. Sci. 256 (2010) 2672-2679.

[33] J. I. Langford, A. J. C. Wilson, Scherrer after sixty years: A survey and some new results in the determination of crystallite size, J. Appl. Cryst. 11 (1978) 102-113.

[34] D. Mardare, G. I. Rusu, The influence of heat treatment on the optical properties of titanium oxide thin films, Mater. Lett. 56 (2002) 210-214.

[35] *Semiconductor Electrodes, Studies in Physical and Theoretical Chemistry,* edited by H. O. Finklea, Elsevier Science, Amsterdam, 1988, Vol. 56.

Figure captions

Figure 1 SEM images of as-anodized TiO_2 nanotubular layers showing (a) top-view (b) cross-sectional view.

Figure 2 SEM top-view images of TiO_2 nanotubular layers annealed at (a) 300 ^oC, (b) 400 ^oC, (c) 500 ^oC and (d) 600 ^oC for 3 h. The scale bars represent the distance of 100 nm.

Figure 3 Cross-sectional SEM images of annealed TiO_2 nanotubular layers. The scale bars represent the distance of 100 nm.

Figure 4 XRD patterns of TiO_2 nanotube layers annealed at different temperatures.

Figure 5 IPCE spectra measured at 0.4V (vs Ag/AgCl) using 0.1 (M) Na_2SO_4 solutions for TiO_2 nanotubular layers annealed at (a) 300 ^oC, (b) 400 ^oC, (c) 500 ^oC and (d) 600 ^oC. The insets show $(IPCE.hv)^{1/2}$ vs. hv to identify the change in the bandgaps of layers after being annealed at different temperatures.

Figure 6 (a) Resistance of the annealed TiO_2 nanotubular layers measured using conducting AFM and two-point probe technique, (b-c) schemes of contact areas between the nanotube layers annealed at 300 °C and 600 °C and tips used for conductivity measurements; (d-e) SEM images of corresponding TiO_2 nanotube layers showing different roughness of the uppermost nanotube parts.

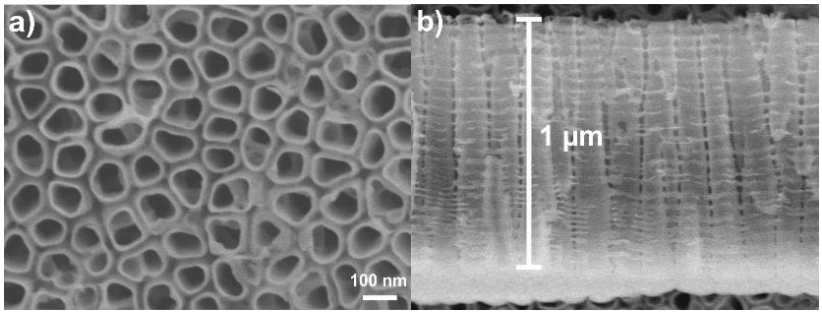

Figure 1

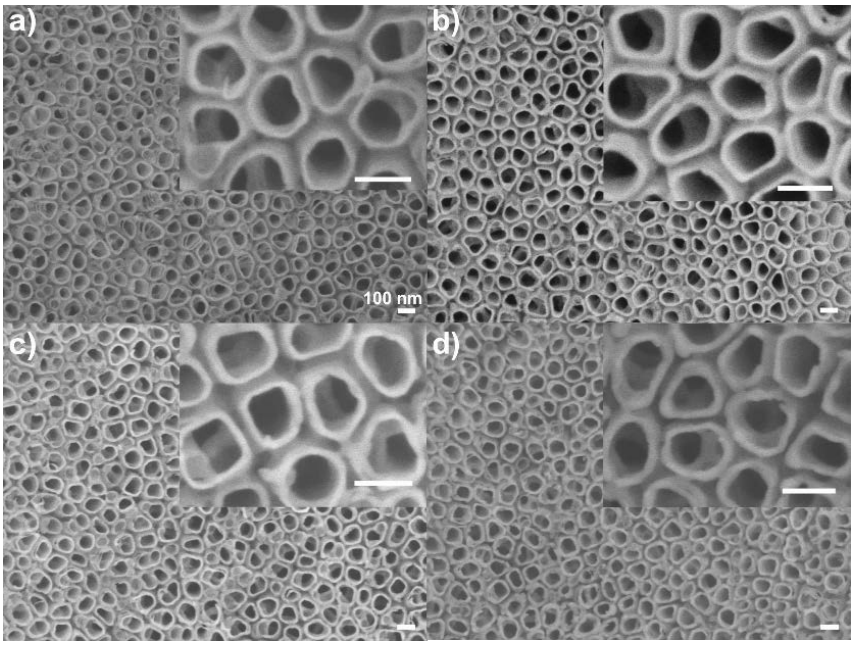

Figure 2

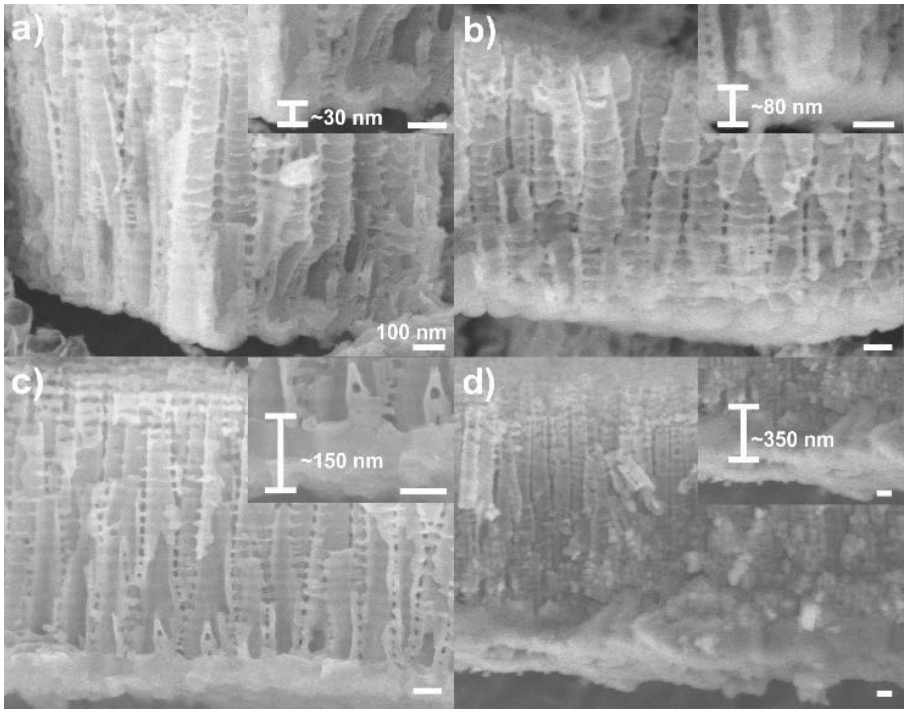

Figure 3

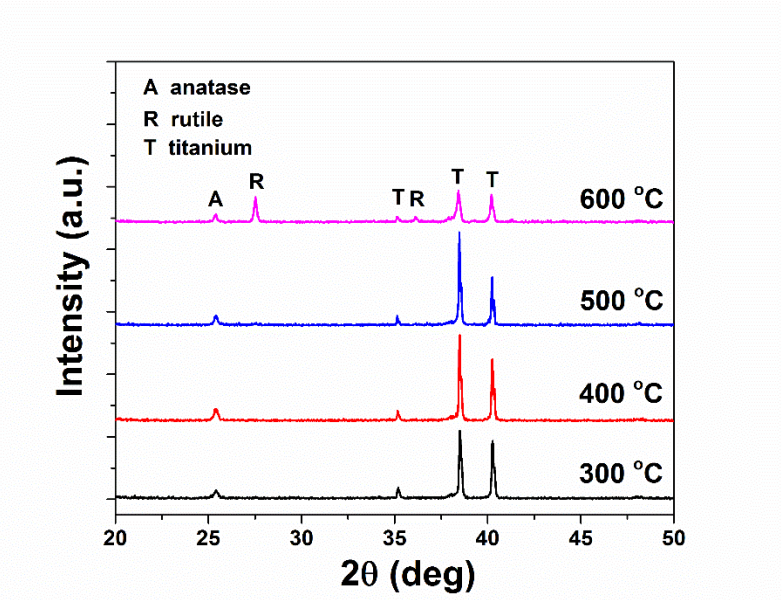

Figure 4

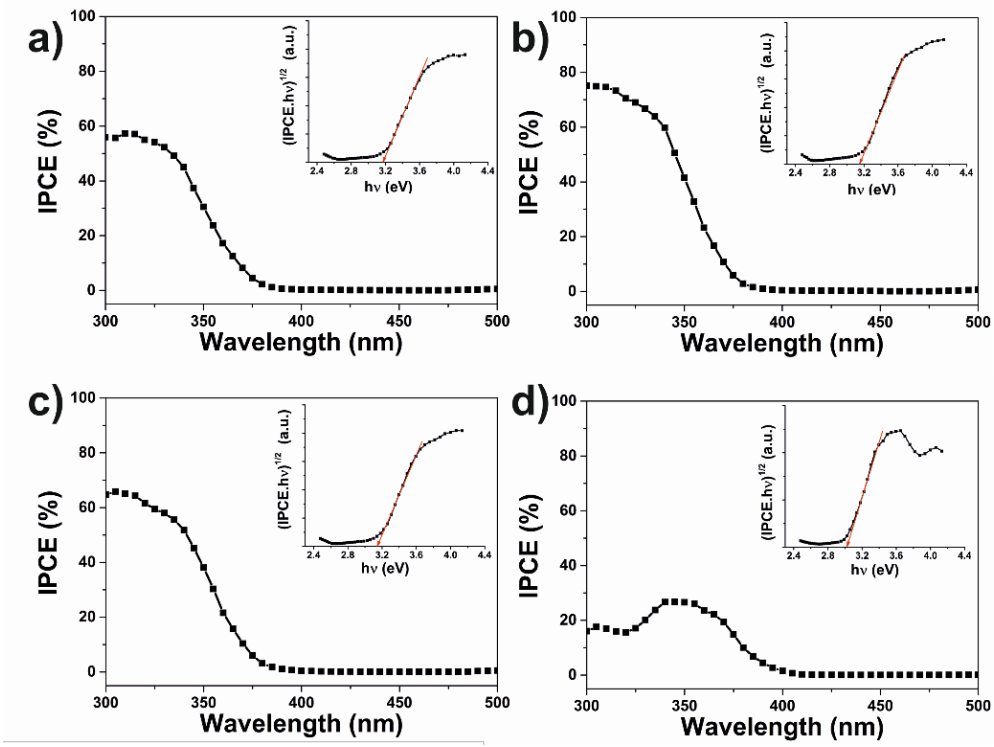

Figure 5

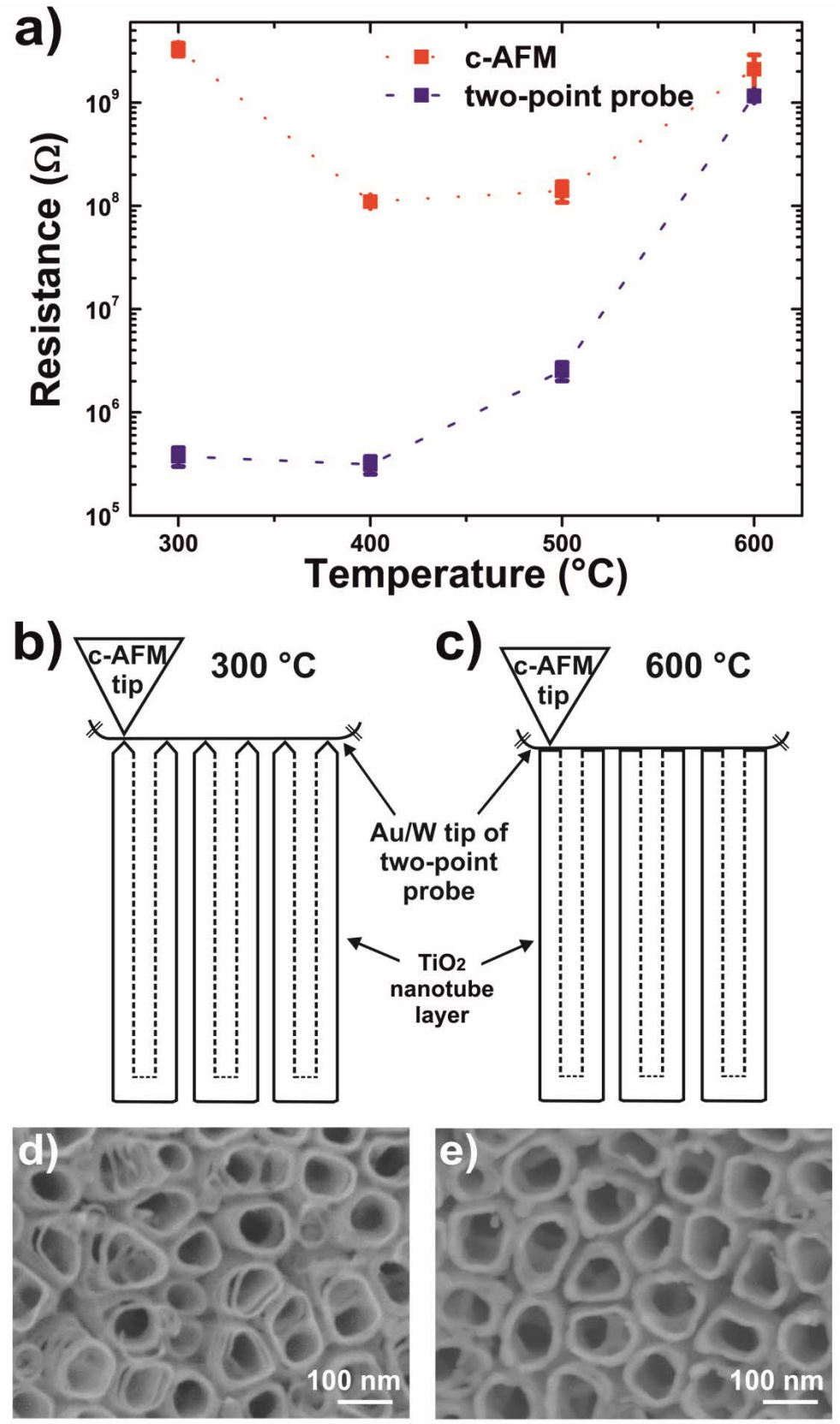
a)
c-AFM
two-point probe
Resistance (Ω)
10^9
10^8
10^7
10^6
10^5
300
400
500
600
Temperature (°C)
b)
c-AFM tip
300 °C
c)
c-AFM tip
600 °C
Au/W tip of two-point probe
TiO2 nanotube layer
d)
100 nm
e)
100 nm

Figure 6

Table 1 Comparison of bandgap, anatase and rutile grain size for 1 μm thick TiO_2 nanotube layer annealed at different temperatures

Annealing Temperature	**Bandgap (eV)**	**anatase crystallite size (nm)**	**rutile crystallite size (nm)**
300 ^{o}C	3.19	35.3	-
400 ^{o}C	3.16	34.7	-
500 ^{o}C	3.14	48.5	-
600 ^{o}C	3.02	50	61.5